

Thermal map detection method for web page based on thermopile array sensor

Fan Yang*, Jun Xu[#]

Department of Automation, Faculty of Automation, Harbin University of Science and Technology, Harbin, Heilongjiang, China

ABSTRACT

In this paper, a monitoring system based on thermopile array sensors is designed for real-time refreshing of thermograms in a web interface. To address the problem of inconspicuous heat map of the main target caused by the interference of the detection environment and the small temperature difference between the target to be measured and the background, a dynamic color mapping processing scheme is proposed to make the heat map of the main target displayed more clearly by continuously adjusting the contrast between the main target and the background color. The experimental results show that the method can achieve dynamic refreshing of the thermogram through a multi-device browser, the correlation of measurement data is greater than 85% compared to handheld thermometers, and the effective transmission distance is about 30m in open range, which can effectively enhance the portability and safety of staff during COVID-19 temperature screening.

Keywords: COVID-19, thermopile array sensor, infrared heat map, web monitoring

1. INTRODUCTION

Non-contact temperature measurement is an important method to determine temperature not only in industrial testing but also in people's daily life. Especially in the serious pandemic, this method has more safety and convenience advantages than contact temperature measurement.

There are many methods of non-contact temperature measurement, including common forehead temperature gun and ear thermometer in life, the principle of which is to collect the infrared radiation from the measured object to the photoelectric detector, and convert the light signal into an electrical signal, and finally get the temperature value of the measured target after data processing, but this way is commonly used in the temperature measurement scenario of a single point location, and cannot provide feedback on the temperature of the whole profile¹. Currently in enterprises and institutions is based on infrared camera with computers to complete the dynamic heat map monitoring. Although this approach has excellent refresh rates and accuracy, it is less portable and relies on a strong computer performance in scenarios where the location needs to be changed frequently². Based on the above problems, the aim of this paper is to propose a thermal map web detection method based on thermopile array sensors for human body temperature measurement in some scenarios where frequent movement is required, to enhance the portability of the device and to reduce the cost of infrared sensors in abnormal temperature screening, the contribution of this paper is twofold.

(a) A thermogram web detection method based on thermopile array sensors is proposed to optimize due to the size, volume, and cost caused the low-resolution, not portable, and high-cost problems. The problems of low resolution, portability, and high cost of previous devices due to the size, volume, and cost of the display screen.

(b) In terms of enhancing the display of web pages, a method of dynamic color mapping of temperature matrices is proposed to optimize the poor effect of heat maps caused by the influence of disturbing heat sources and ambient temperature differences.

2. SENSOR DETECTION SYSTEMS

The entire detection system is shown in Figure 1. The system consists of a web server consisting of sensors and microcontrollers, a Wi-Fi router and terminals. After connecting the hardware board to the Wi-Fi network, the users can

*yf45619@gmail.com; #xujun@hrbust.edu.cn

access the IP address of the web server using the browser of the mobile device within the same network, and complete the task of real-time monitoring of the portrait heat map.

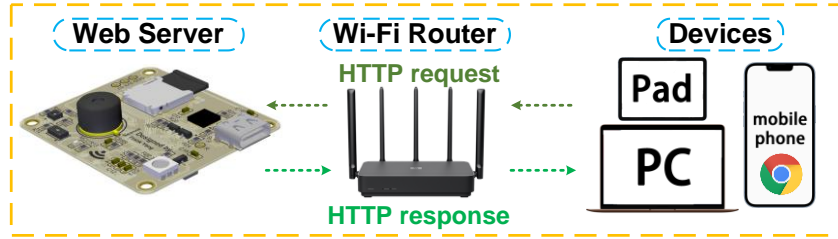


Figure 1. Integral inspection system.

The hardware board is shown in Figure 2. It mainly includes Melexis MLX90640ESF-BAB thermopile array sensor, and the temperature range of targets is -40°C - 300°C , ESP32-Pico-D4 dual-core microprocessor, Micro SD card, CP2102 serial communication chip, PSRAM chip, RGB LED, AMS1117 buck chip, etc.³. The board features a USB Type-C 5V voltage input, is approximately 43.3mm wide and 38.6mm high, and the four corners can be secured with M3 size screws.

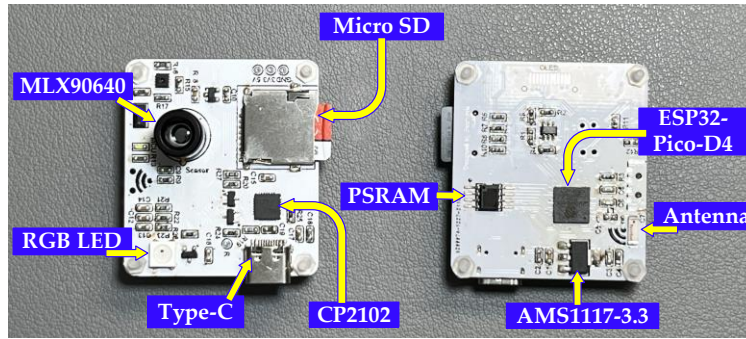


Figure 2. Hardware development board layout.

3. OPTIMISATION OF DATA PROCESSING AND DISPLAY PROCESSES

The process from the acquisition of raw sensor data followed by temperature conversion to the interpolation algorithm and dynamic color mapping of the heat map in the web interface is shown in Figure 3.

3.1 Raw data acquisition and temperature conversion

When the sensor is in operation, the results of the infrared radiation are continuously stored in the ram at different addresses via the sensor's independent amplifier and ADC⁴. The microprocessor can complete the scanning of the data in the different addresses for acquisition by means of I²C communication. The process of converting the data in the addresses into temperature data is calculated as:

$$T_1(i, j) = \sqrt[4]{\frac{V_{IR(i,j)}}{\alpha_{comp(i,j)} \times ALpha_{corr} \times (1 + Ks_{TOX} \times (T_{0(i,j)} - CT_X))}} + T_{a-r} - 273.15 \quad (1)$$

where (i,j) is the coordinates of the pixel point acquired by the sensor, $T_1(i,j)$ is the temperature parameter of the pixel point, $V_{IR(i,j)}$ is the radiance compensation coefficient of the pixel point, $\alpha_{comp(i,j)}$ is the normalized sensitivity coefficient of the pixel point, $ALpha_{corr}$ is the sensitivity correction coefficient for different ranges, Ks_{TOX} is the sensitivity slope for different ranges, CT_X is four different temperature ranges of -40°C , 0°C , 160°C , and 320°C , and T_{a-r} is the temperature signal reflected by the object, which can be calculated from the ambient temperature and the reflection coefficient.

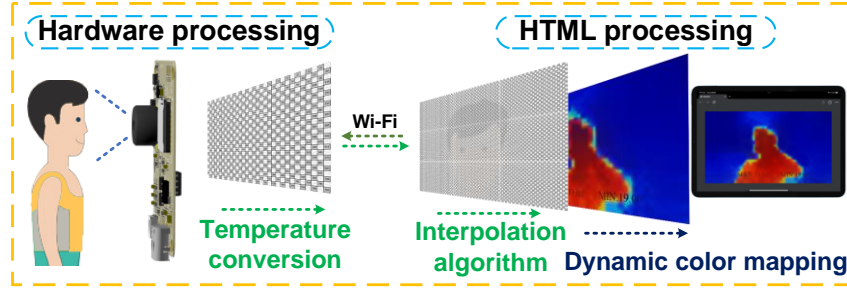


Figure 3. Interpolation process and dynamic color mapping process for heat maps.

3.2 Calculation of interpolation of temperature matrix

Considering the performance of the microprocessor and the real-time nature of data transmission, as well as the fact that there is less high-frequency information in the heat map when detecting human images, and given that the bilinear interpolation algorithm has relatively impressive performance in terms of operational efficiency, memory consumption and interpolation effect. This paper chooses to carry out the bilinear interpolation algorithm in the web page for the 768 pixel points obtained for image quality. This not only guarantees the real-time performance of hardware and web page data transmission but also reduces the power consumption of the microprocessor, allowing more processing to be completed in the browser of the mobile device. This algorithm has also been used in many microprocessor-based image processing projects^{5,6}.

The interpolation algorithm process is shown in Figure 4. Although the temperature parameter corresponding to the new co-ordinate point after the image has been enlarged is unknown, the number of times the image needs to be enlarged is known. After the new coordinate points are mapped, the actual pixel points in the immediate vicinity are determined based on the current point information, and two single linear interpolations are performed in the y -direction to obtain Z_1 and Z_2 points, and one single linear interpolation is performed in the x -direction to obtain Z point $f(x,y)$.

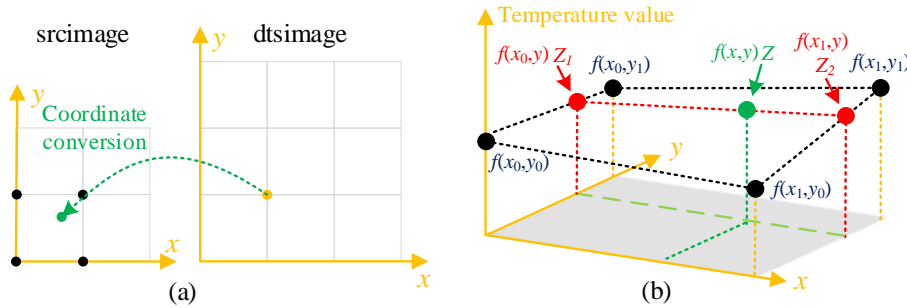


Figure 4. (a) Coordinate conversion process; (b) Interpolation calculation process.

$$f(x, y) = (x_1 - x) \times [f(x_0, y_0) \times (y_1 - y) + f(x_0, y_1) \times (y - y_0)] + (x - x_0) \times [f(x_1, y_0) \times (y_1 - y) + f(x_1, y_1) \times (y - y_0)] \quad (2)$$

where $f(x_0, y_0)$, $f(x_0, y_1)$, $f(x_1, y_0)$, $f(x_1, y_1)$ are the temperature values of the known neighboring pixel points at the mapped coordinates, and x_0, y_0, x_1, y_1 are the known neighboring pixel point coordinates.

3.3 Dynamic color mapping for heat maps

In order to convert the temperature data into a heat map in the web interface, a dynamic color mapping method for heat maps is proposed, which can effectively display the temperature matrix in the form of a heat map on the web page with a dynamic refresh. The backend processing of the web page is shown in Figure 5.

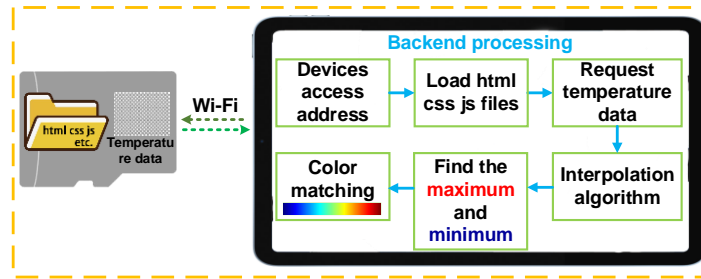


Figure 5. Backend processing of web page.

Achieving effective color mapping of temperature data is a key aspect of a high-quality display of heat maps. In previous work, the colors were mapped to different temperatures and thus the images were stitched together, but in some scenes where there is little difference in temperature between the human body and the background or where there are many background disturbing heat sources, the portrait display is not obvious. In this paper, a dynamic color mapping method is proposed with the aim of obtaining higher contrast and better imaging results, the mapping process is shown in Figure 6.

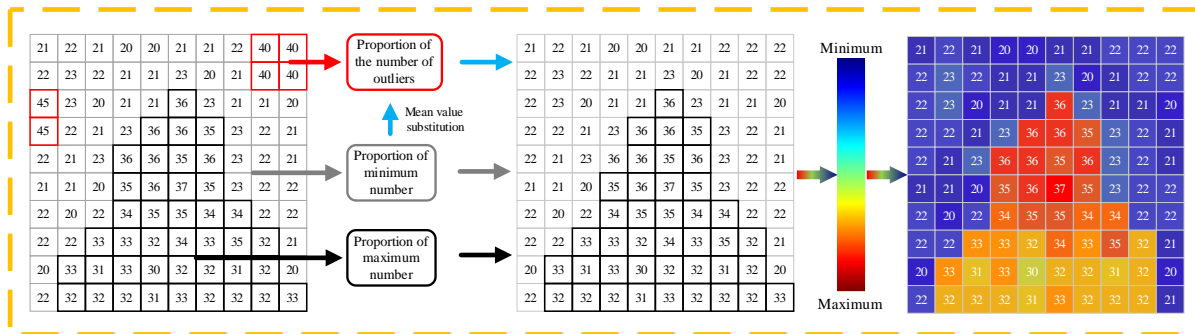


Figure 6. Dynamic color mapping process.

As we known from the figure above, after performing the temperature data interpolation operation, the temperature values are traversed for all pixel points and the number of maximum and minimum values as well as the number of pixel points with similar temperature values in adjacent areas are counted and their ratio to the number of all pixel points is calculated, in proportion to the transition from red to blue^{7,8}. When there are multiple points of interfering heat sources in the background, by setting a threshold and counting the number of abnormal temperature points and the number of pixel points with similar temperature values in adjacent areas, the ratio of the calculator is calculated and the average value of the temperature of all pixel points within the minimum value is used to replace the interfering pixel point value to achieve the effect of filtering the background of interfering heat sources and improve the display quality⁹. The comparative results of the different treatment methods are shown in Figure 7.

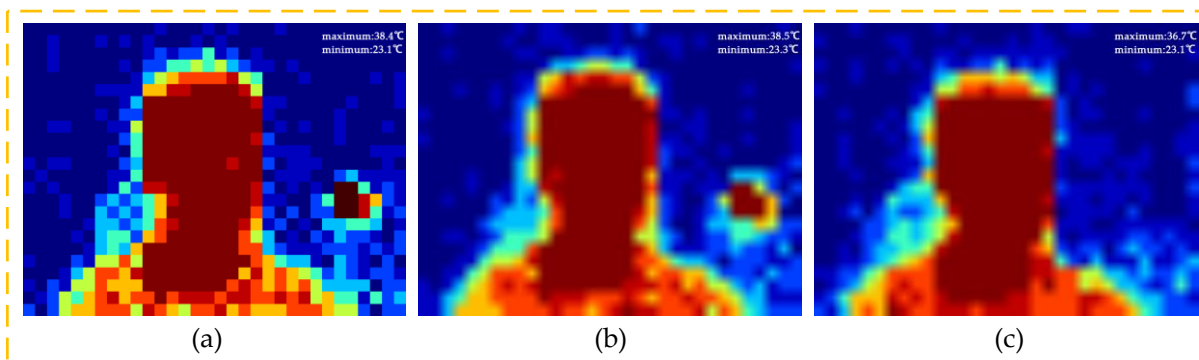


Figure 7. Comparative results of different treatment methods (a) Results not processed by interpolation algorithm (b) Result of interpolation algorithm (c) Interference point anomaly handling results

4. DATA ACCURACY ANALYSIS

The experimental scenario is shown in Figure 8. In order to verify the accuracy of the device's temperature measurement, a thermometer and the device in this paper were used in the experiment to work simultaneously at a distance of 0.5m from the human body, at a room temperature of 25°C, and the temperature was measured every 5 minutes for one consecutive hour¹⁰, with the mobile monitoring device being a tablet, and both the device and the tablet connected to the Wi-Fi of the same router. Figure 9 shows the results of the simultaneous temperature detection using the thermometer and the device in this paper within 1 hour comparison results. The results show that the device has a high accuracy of measurement, and the correlation of the data is greater than 85%.

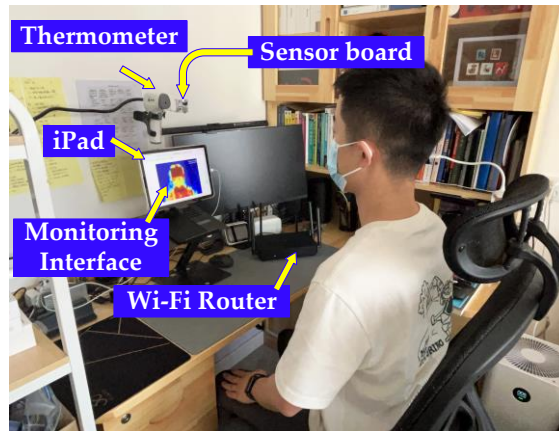


Figure 8. Experimental scene.

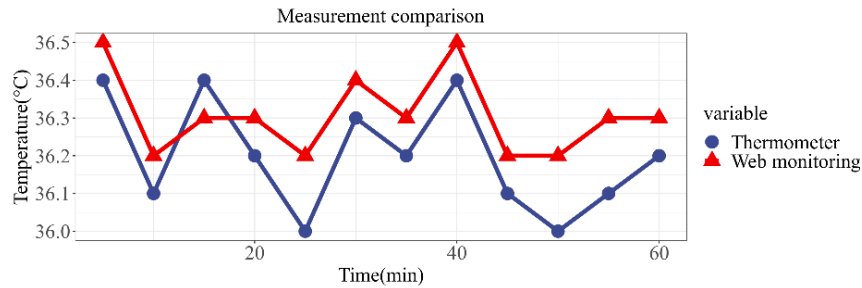


Figure 9. Measurement accuracy comparison curves.

In order to verify the stability of the data transmission, the following experiments were done in this paper. By constantly moving the router location and recording the signal reception strength RSSI at different locations in the background of the webpage, and compare the integrity of the temperature matrix in the hardware and web parts. To exclude chance errors, the signal strength and completeness at each location were averaged over five calculations and the data results are shown in Figure 10.

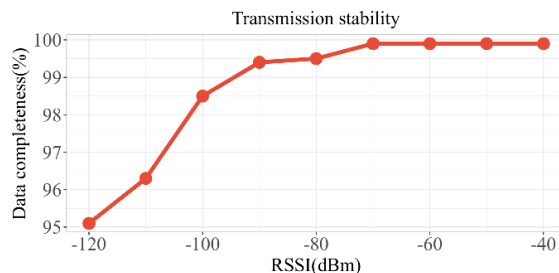


Figure 10. Data transfer stability curves.

As can be seen in Figure 10, there is a direct relationship between Wi-Fi signal strength and data transmission integrity. When the signal strength is below -80dBm, the integrity drops rapidly and data loss is severe. When the signal strength is

close to -80dBm, the open distance between the device and the router is about 30m, which basically meets the usage requirements. In the future, in-depth optimization of the antenna link can also be done in the hardware circuit board section to enhance the integrity of data transmission by improving RF performance.

Combined with relevant experimental data and actual observations, the color dynamically mapped thermogram is clearer and more intuitive, as well as the system information interface makes it easy for the relevant personnel to query the signal strength and memory capacity of the device, and the browser monitoring interface is shown in Figure 11.

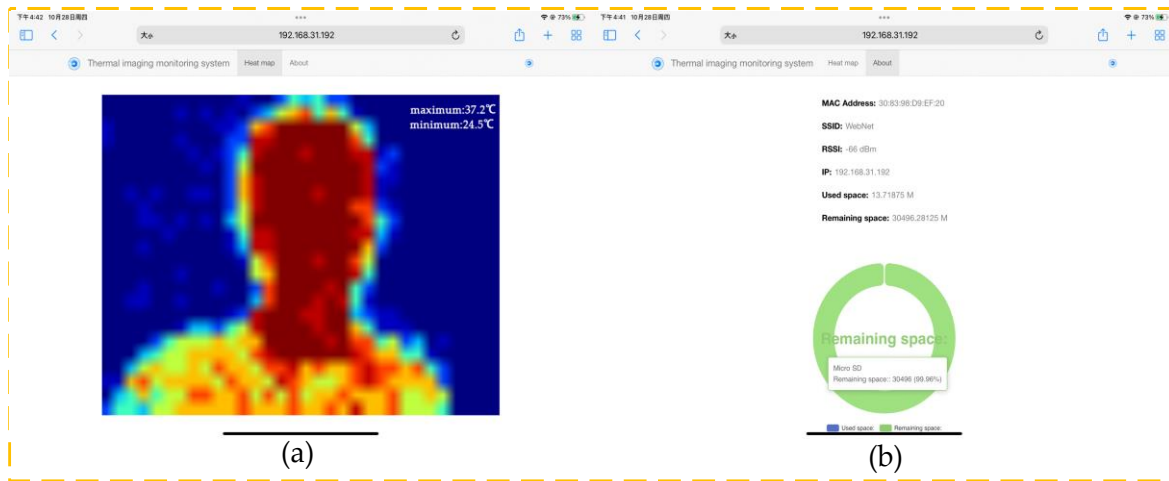


Figure 11. Browser monitoring interface: (a) heat map interface; (b) about interface.

5. CONCLUSIONS

This paper presents a thermogram web detection method based on thermopile array sensors, which enables the detection of human body temperature thermograms via a web interface through interpolation algorithms and dynamic color mapping of temperature data. The detection system designed in this paper has a high degree of data correlation compared to handheld thermometers, and the thermogram display is more intuitive and supports simultaneous monitoring by multiple devices, making it simpler and more portable for frontline medical staff to operate, and safer than manual measurements to avoid contact. This work has also served as a reference for some wireless sensor monitoring.

REFERENCES

- [1] Ng, D. K. K., Chan, C. H., Chan, E. Y. T., Kwok, K. L., Chow, P. Y., Lau, W. F. and Ho, J. C. S., "A brief report on the normal range of forehead temperature as determined by noncontact, handheld, infrared thermometer," *American Journal of Infection Control*, 33, 227-229 (2005).
- [2] Gutschwager, B., Cardenas-Garcia, D. and Hollandt, J., "Determination of the responsivity non-uniformity of an infrared camera with regard to the measurement of radiance temperatures," *Measurement Science & Technology*, 26, 115402 (2015).
- [3] Liang, F., Cai, C. H., Zhang, K., et al., "Infrared gesture recognition system based on near sensor computing," *IEEE Electron Device Letters*, 42, 1053-1056 (2021).
- [4] Kapas, K., Bozoki, T., Dalya, G., Takatsy, J., Meszaros, L. and Pal, A., "Attitude determination for nano-satellites—I. spherical projections for large field of view infrasensors," *Experimental Astronomy*, 51, 515-527 (2021).
- [5] Adiyasa, I. W., Prasetyono, A. P., Yudianto, A., Begawan, P. P. W. and Sultantyo, D., "Bilinear interpolation method on 8x8 pixel thermal camera for temperature instrument of combustion engine," *Journal of Physics Conference Series*, 1700, 012076 (2020).
- [6] Liu, Y. X., Wei, H. F., Zhang, H. J. and Long, K. P., "Above-threshold queries of environmental conditions based on bilinear interpolation in wireless sensor networks," *Sensors*, 18, 4203 (2018).

- [7] Zhang, Y. and Yang, B., "Traffic flow detection using thermopile array sensor," *IEEE Sensors Journal*, 20, 5155-5164 (2020).
- [8] Wu, S. C., Tzou, J. C. and Ding, C. Y., "A low-cost system for measuring wind speed and direction using thermopile array and artificial neural network," *Applied Sciences*, 11, 4024 (2021).
- [9] Rajmanova, P., Nudzikova, P. and Vala, D., "Application and technology of thermal imagine camera in medicine," *IFAC-PapersOnline*, 28, 492-497 (2015).
- [10] Dell'Isola, G. B., Cosentini, E., Canale, L., Ficco, G. and Dell'Isola, M., "Noncontact body temperature measurement: Uncertainty evaluation and screening decision rule to prevent the spread of Covid-19," *Sensors*, 21, 346 (2021).